Supporting Information for

Insights into the Biotransformation of 2,4,6-Trinitrotoluene by the Old Yellow Enzyme Family of Flavoproteins. A Computational Study

Zhilin Yang,[†] *Tong Wei,*[†] *Hui Huang,*[†] *Hong Yang,*[†,‡] *Yang Zhou,*[†,*] *and Dingguo Xu* [‖,*]

[†] Institute of Chemical Materials, China Academy of Engineering and Physics, 621900 Mianyang, China;

[‡] School of Material Science and Engineering, Tsinghua University, Beijing 100084, China;

[‖] MOE Key Laboratory of Green Chemistry & Technology, Sichuan University, Chengdu 610064, China.

*To whom correspondence should be addressed: E-mail: zhouy@caep.cn (Y. Zhou); dgxu@scu.edu.cn (D. Xu).

Captions

Figure S1. Docking results of TNT ligand in active sites for the initial structure of all MD simulations.

Figure S2. RMSD curves for the protein backbone atoms of all enzymes.

Figure S3. The radius of gyration for all the five wild-type enzymes.

Figure S4. The dihedrals along with the shortest transfer distances between $FMNH_2$ and TNT in (a) MR and (b) OYE.

Figure S5. Non-Covalent Interactions (NCI) results of TNT and some key residues (including $FMNH_2$) of a) PETNR, b) XenR, c) N182H and d) OYE.

Figure S6. The conformation evolution of TNT and key residues of *a)* PETNR, and *b)* H184N in the range of the initial non-equilibrium simulation time; and the curves of non-bonded interaction energy of key residues with TNT in active sites.

Figure S7. The conformation evolution of TNT and key residues of *a)* XenR, and *b)* N175H in the range of the initial non-equilibrium simulation time; and the curves of non-bonded interaction energy of key residues with TNT in active sites.

Table S1. PDB codes and simulation model information for five wild-type enzymes.

Table S2. Average distances and standard deviations between transferred hydrogen atoms (H_{20} or H_{21}) and TNT reaction sites (C_3, C_5, O_1-O_6) at the last 10 ns equilibrium simulation time for five wild-type enzymes. (Distance in Å)

Table S3. Average distances and standard deviations between transferred hydrogen atoms (H_{20} or H_{21}) and TNT reaction sites (C_3, C_5, O_1-O_6) at the last 10 ns equilibrium simulation time for five mutants. (Distance in Å)

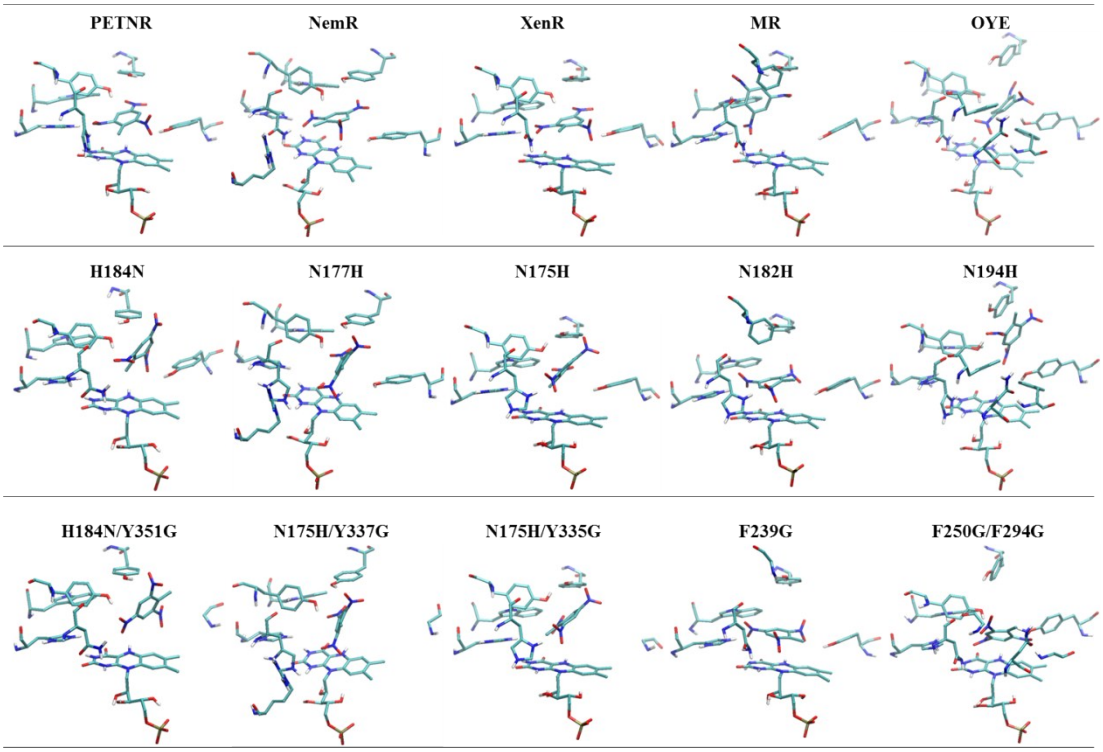

Figure S1. Docking results of TNT ligand in active sites for the initial structure of all MD simulations.

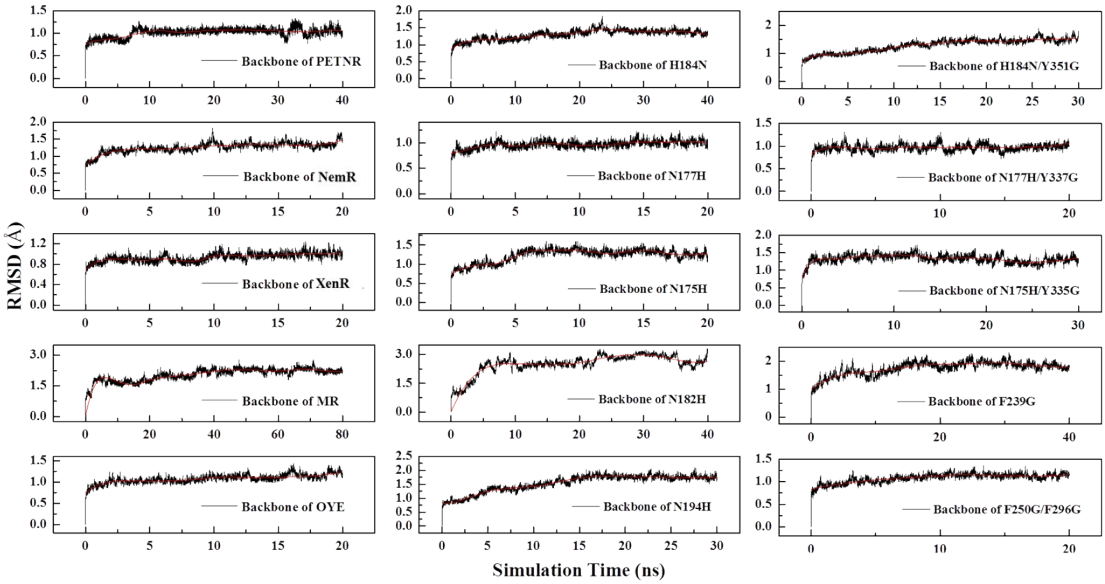

Figure S2. RMSD curves for the protein backbone atoms of all enzymes.

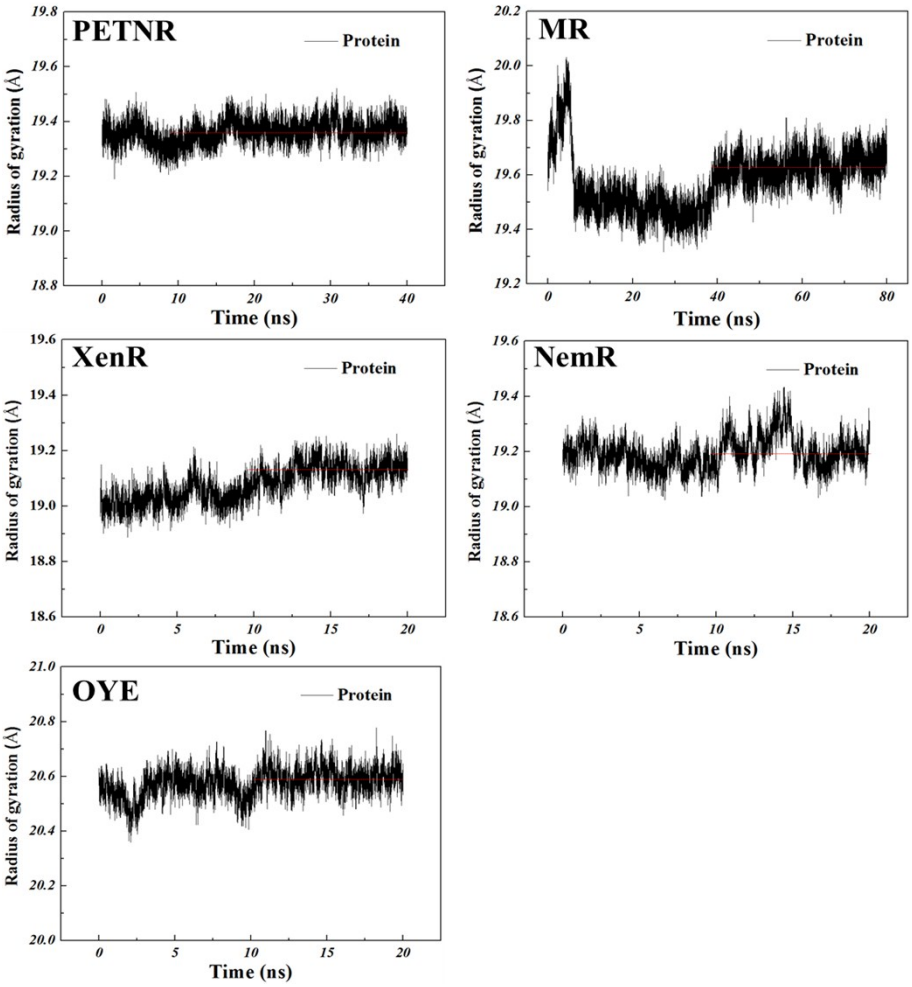

Figure S3. The radius of gyration for all the five wild-type enzymes.

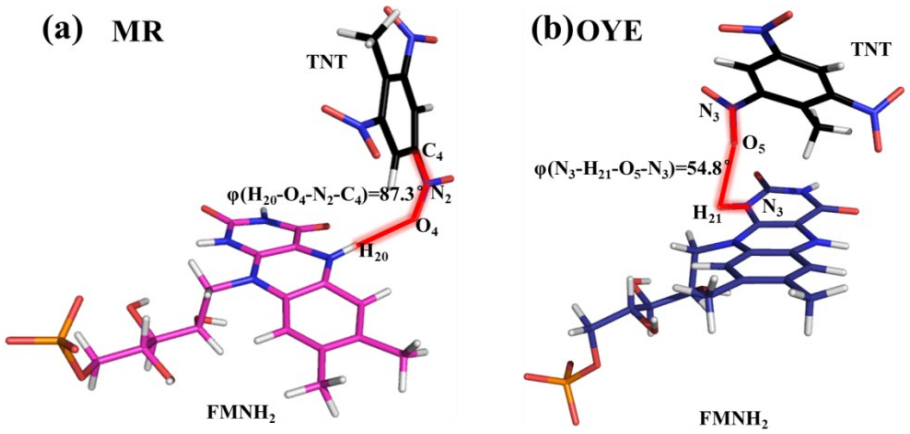

Figure S4. The dihedrals along with the shortest transfer distances between $FMNH_2$ and TNT in MR (a) and OYE (b).

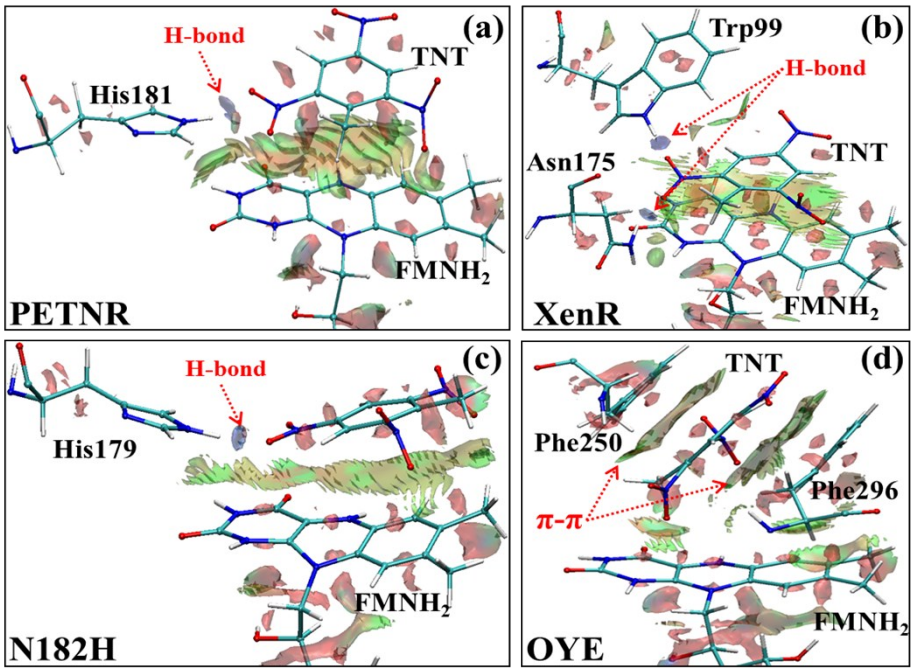

Figure S5. Non-Covalent Interactions (NCI) results of TNT and some key residues (including $FMNH_2$) of a) PETNR, b) XenR, c) N182H and d) OYE.

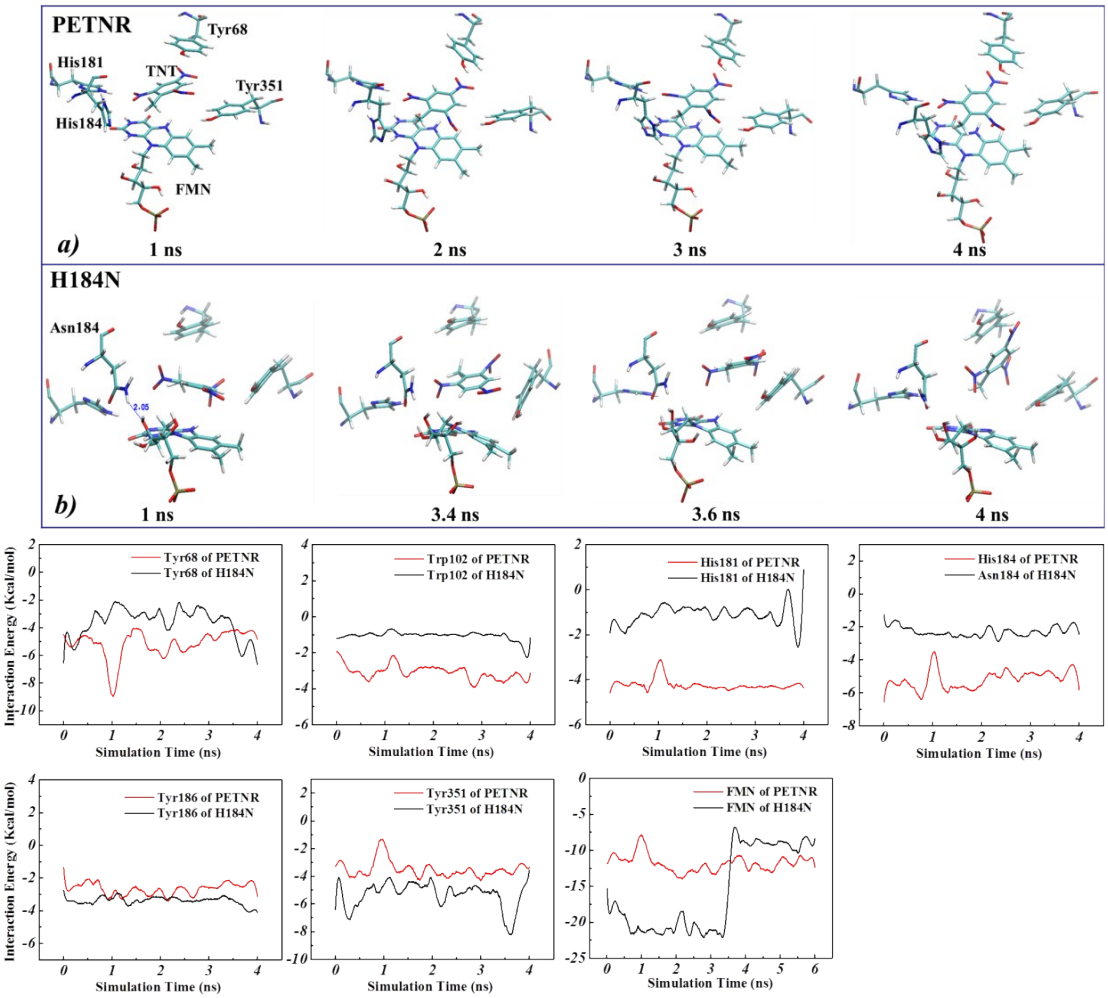

Figure S6. The conformation evolution of TNT and key residues of *a)* PETNR, and *b)* H184N in the range of the initial non-equilibrium simulation time; and the curves of non-bonded interaction energy of key residues with TNT in active sites.

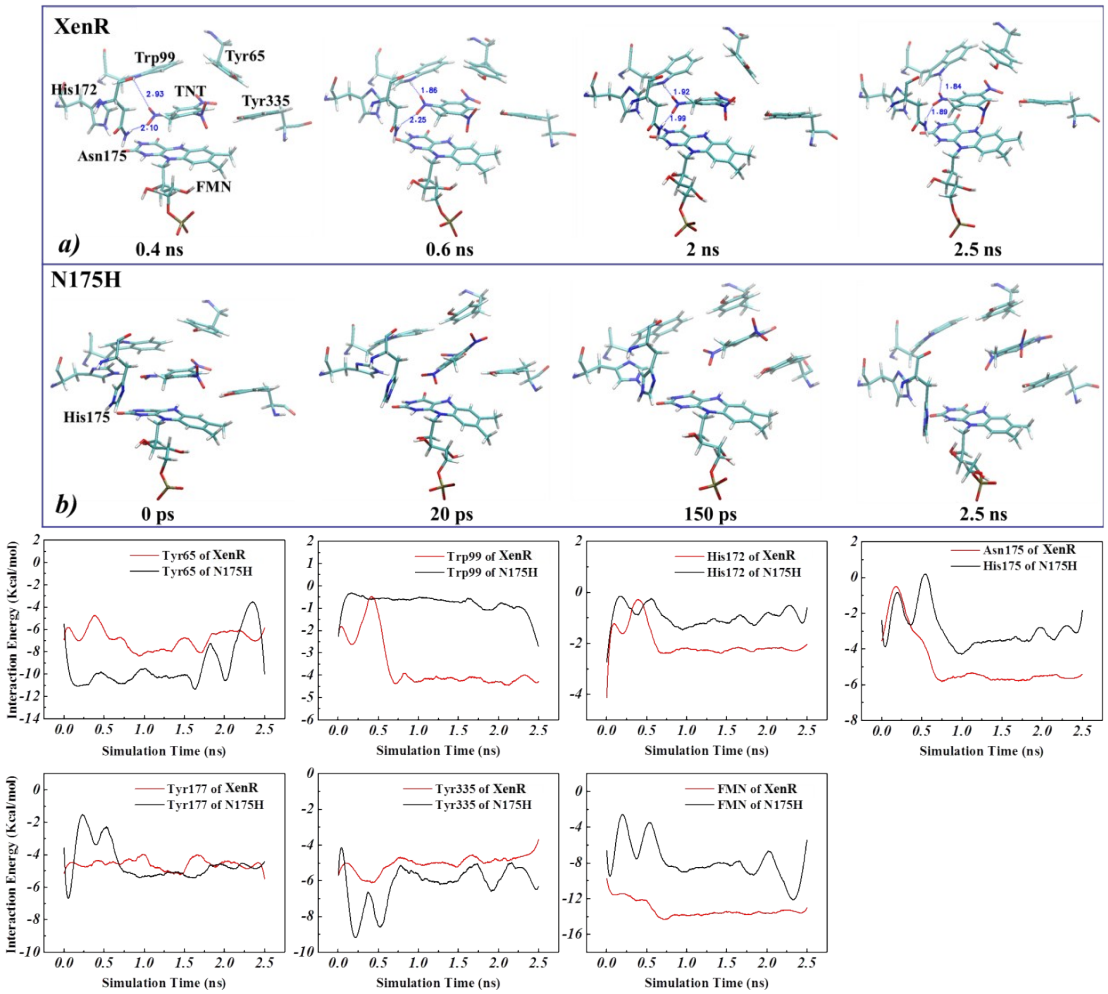

Figure S7. The conformation evolution of TNT and key residues of *a)* XenR, and *b)* N175H in the range of the initial non-equilibrium simulation time; and the curves of non-bonded interaction energy of key residues with TNT in active sites.

Table S1. PDB codes and simulation model information for five wild-type enzymes.

Enzyme	Abbreviation	PDB code	Box Size/Å	Number of protein/cofactor/TNT/Na^+/water atoms
Pentaerythritol tetranitrate reductase	PETNR	1GVR	92×74×94	5510/52/21/9/47196
N-Ethylmaleimide reductase	NemR	3GKA	91×75×81	5239/52/21/7/39852
Xenobitotic reductase B	XenR	4AB4	86×83×82	5281/52/21/9/42159
Morphinone reductase	MR	2R14	86×84×91	5516/52/21/14/47571
Old yellow enzyme	OYE	1OYA	98×85×77	6271/52/21/6/47481

Table S2. Average distances and standard deviations between transferred hydrogen atoms (H_{20} or H_{21}) and TNT reaction sites (C_3, C_5, O_1-O_6) at the last 10 ns equilibrium simulation time for five wild-type enzymes. (Distance in Å)

		C_3	C_5	O_1	O_2	O_3	O_4	O_5	O_6
PETNR	H_{20}	3.29±0.25	3.77±0.32	4.38±0.43	4.79±0.45	4.66±0.34	4.59±0.26	5.13±0.55	5.67±0.62
	H_{21}	6.20±0.27	7.11±0.32	4.84±0.40	4.86±0.60	9.21±0.29	8.77±0.26	6.66±0.69	7.55±0.70
NemR	H_{20}	3.80±0.35	4.27±0.77	5.15±0.72	5.36±0.78	4.31±1.01	4.48±0.80	6.13±1.31	6.13±1.24
	H_{21}	5.32±0.50	6.27±0.72	4.94±1.41	4.33±1.76	7.03±1.39	7.24±1.63	7.22±1.37	7.13±1.45
XenR	H_{20}	3.30±0.25	3.95±0.30	5.14±0.51	5.03±0.46	3.92±0.35	3.83±0.36	6.17±0.56	6.04±0.57
	H_{21}	5.83±0.32	6.99±0.38	4.29±0.63	4.35±0.64	8.58±0.39	8.08±0.39	7.59±0.75	7.42±0.84
MR	H_{20}	4.51±0.35	5.39±0.28	6.69±0.64	6.70±0.66	3.24±0.94	3.02±0.93	8.12±0.35	8.14±0.36
	H_{21}	8.26±0.51	9.18±0.35	9.08±1.05	9.09±1.09	8.11±0.91	7.90±0.93	11.10±0.53	11.02±0.57
OYE	H_{20}	6.75±0.53	7.26±0.44	5.01±1.19	5.15±1.11	9.47±0.51	9.30±0.57	6.23±0.93	6.97±1.02
	H_{21}	7.78±0.44	6.57±0.39	7.79±1.00	7.90±0.91	8.99±0.54	9.82±0.46	3.84±0.81	4.57±0.82

Table S3. Average distances and standard deviations between transferred hydrogen atoms (H_{20} or H_{21}) and TNT reaction sites (C_3, C_5, O_1-O_6) at the last 10 ns equilibrium simulation time for five mutants. (Distance in Å)

		C_3	C_5	O_1	O_2	O_3	O_4	O_5	O_6
H184N	H_{20}	5.79±0.54	3.73±0.41	7.91±0.56	7.99±0.47	5.26±0.72	5.73±1.16	3.52±1.12	3.29±1.11
	H_{21}	8.18±0.95	6.71±0.54	11.02±0.96	11.10±0.98	5.46±1.06	6.09±1.70	8.07±0.85	7.94±0.86
N177H	H_{20}	5.15±0.58	6.71±0.60	4.65±1.72	4.14±1.72	6.47±1.04	7.14±1.55	8.31±0.78	8.33±0.82
	H_{21}	9.38±0.80	11.05±0.64	7.57±1.09	7.36±1.03	11.30±1.30	11.87±1.80	11.95±0.99	11.92±1.04
N175H	H_{20}	7.77±0.46	5.80±0.48	9.14±0.64	9.04±0.73	8.51±1.07	8.13±1.00	3.89±0.70	3.62±0.80
	H_{21}	11.06±0.68	8.86±0.59	13.23±0.61	13.17±0.71	10.36±1.45	9.87±1.42	7.98±0.92	7.65±1.05
N182H	H_{20}	4.44±0.30	3.44±0.25	6.67±0.56	6.72±0.56	4.39±0.30	3.82±0.34	4.94±0.31	4.62±0.40
	H_{21}	5.75±0.37	6.70±0.28	7.52±0.80	7.60±0.78	3.93±0.34	5.28±0.31	9.33±0.29	9.22±0.35
N194H	H_{20}	4.64±0.38	5.81±0.44	3.12±1.00	3.78±0.97	7.11±0.64	6.94±0.53	6.71±0.55	6.67±0.59
	H_{21}	9.07±0.44	9.37±0.49	7.22±0.94	7.82±0.97	11.57±0.50	11.51±0.47	8.45±0.77	8.46±0.76